

Supplement of Biogeosciences, 13, 5677–5696, 2016
<http://www.biogeosciences.net/13/5677/2016/>
doi:10.5194/bg-13-5677-2016-supplement
© Author(s) 2016. CC Attribution 3.0 License.



Supplement of

Microbial dynamics in a High Arctic glacier forefield: a combined field, laboratory, and modelling approach

James A. Bradley et al.

Correspondence to: James A. Bradley (j.bradley@bristol.ac.uk)

The copyright of individual parts of the supplement might differ from the CC-BY 3.0 licence.

S1. Cell count to volume conversion

Length = h_1

Width = h_2

$$\text{bacterial carbon} = \left(\frac{\pi}{4} \times h_2^2 \times \left(\frac{h_1 - h_2}{3} \right) \right) \times 2.2 \times 10^{-7}$$

(S1)

(Bratbak and Dundas, 1984)

S2. ^3H -Leucine concentration calibration

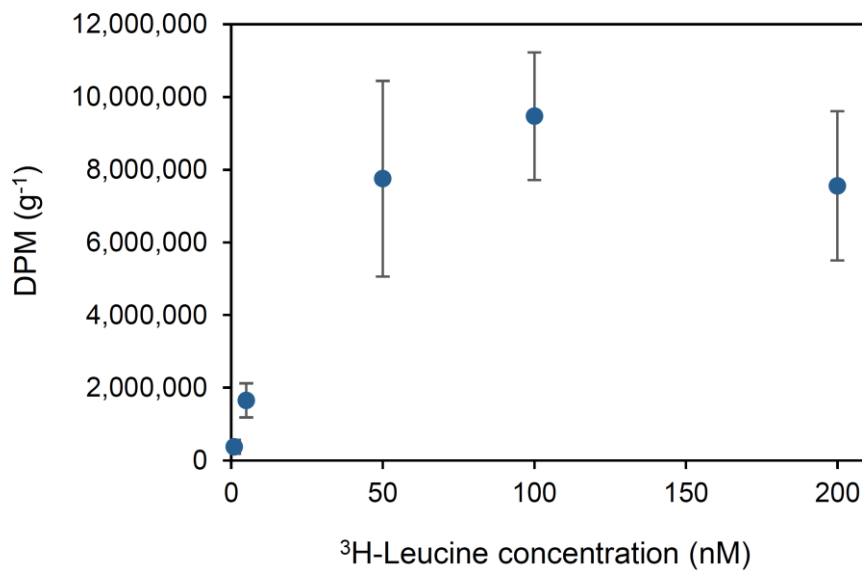


Fig. S1. ^3H -Leucine concentration calibration (error bars show 1 standard deviation).

S3. Model Implementation and set-up

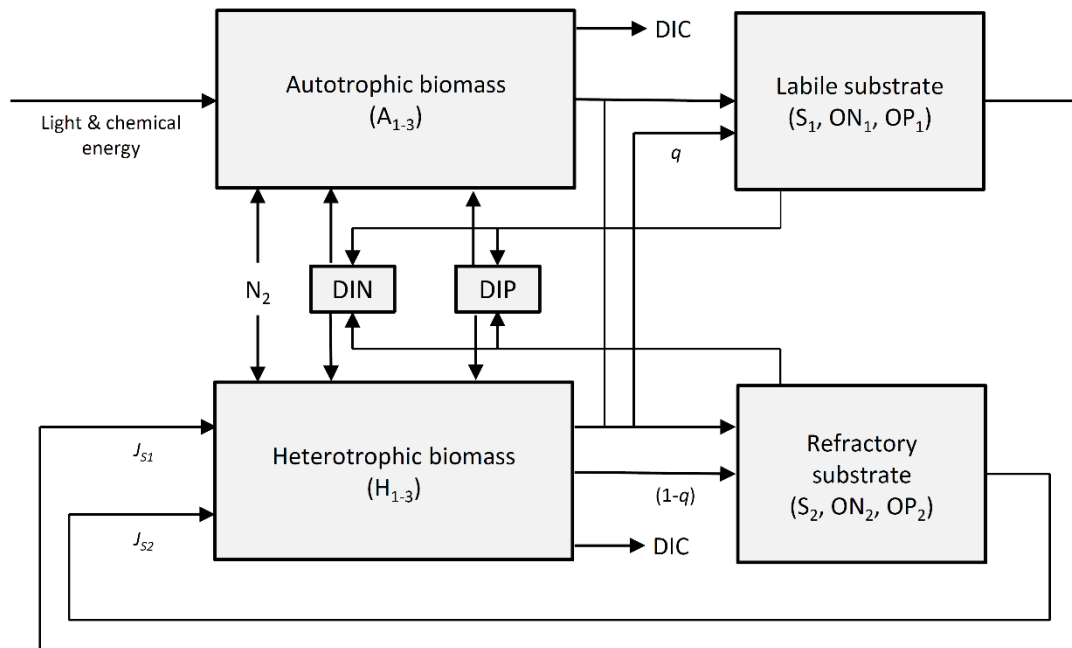


Fig. S2. A conceptual model showing the components and transfers of SHIMMER. State variables are indicated with shading. Image reproduced from Bradley et al. (2015).

S3.1. Initial conditions

Initial conditions are informed by analysis of 0-years-of-exposure soil collected adjacent to the ice snout, and values for all state variables are presented in Table 1. Microbial biomass is estimated by microscopy. Initial community structure is derived by 16S analysis of year-0 soils. An initial value for carbon substrate ($S_1 + S_2$) is estimated based on the average TOC content of year-0 soil (Carlo-Erba NC2500 elemental analyzer). Bioavailability is assumed to be 30% labile (S_1) and 70% refractory (S_2). Organic Nitrogen (ON) and organic Phosphorus (OP) are assumed to be stoichiometrically linked by the measured C:N:P ratio from which the model was initially developed and tested (Bradley et al., 2015). An initial value for DIN is taken from a previous evaluation of biogeochemistry of Svalbard tundra, whereby the lowest value is taken to represent the soil of least development, according to traditional understanding of forefield nutrient dynamics (Alves et al., 2013; Bradley et al., 2014). An initial value for DIP is established stoichiometrically from previous model development and testing.

S3.2. Forcing data

The following external forcings drive and regulate the system's dynamics:

- Photosynthetically-active radiation (PAR) (wavelength of approximately 400 to 700nm) ($W m^{-2}$).
- Snow depth (m).
- Soil temperature ($^{\circ}C$).
- Allochthonous inputs ($\mu g g^{-1} d^{-1}$).

Soil temperature (at 1cm depth) for the entire of 2013 is provided by AWI from the permafrost observatory near Ny-Ålesund, Svalbard. Similarly, PAR for 2013 is measured at the AWI meteorological station near Ny-Ålesund, Svalbard. Averaged daily snow depth for 2009 to 2013 is provided by the Norwegian Meteorological Institute (eKlima). The presence of snow on the ground attenuates sunlight and inhibits PAR from reaching the soil surface. This is accounted for in pre-processing of forcing data. Light attenuation is estimated according to the equation:

$$n = n_0 e^{-mx} \quad (S2)$$

Whereby n is the irradiance (W/m^2), x is the snow depth (m) and m is the extinction coefficient for snow. The extinction coefficients for various types of snow can be measured and an estimate of 6 is used in this instance to represent snow in the Midtre Lovénbreen forefield (Greenfell and Maykut, 1977). Due to its high latitude, the study site experiences continual daylight for much of the summer and continual darkness for much of the winter. Forcing data is provided as daily averages, and linear interpolation is used between any (very infrequent) missing data points.

Allochthonous inputs are estimated based on the best available budget of catchment hydrology and nutrients for Midtre Lovénbreen presented in Hodson et al. (2005). Data from two summer-winter seasons allow nutrient deposition, runoff and retention to be estimated. In SHIMMER, prescribed inputs (I) are only partially retained (v). v_{DIN} is equal to the average of the residual (retained) DIN divided by the total DIN deposition flux over the two years of observations. The retention flux is assumed to be equal for all nutrient species ($v_{DIN} = v_{Sub} = v_{DIP}$) and this allows the total deposition of DIP to be back-calculated from the runoff flux.

$$v_{DIN} = \frac{\text{retainment}}{\text{inputs (snow \& rain)}} \quad (S3)$$

Table S1. v-values

Variable	Value
<i>VNO3 1999</i>	0.146
<i>VNH4 1999</i>	-0.056
<i>VNO3 2000</i>	-0.089
<i>VNH4 1999</i>	0.688
average <i>vDIN</i>	0.172

I_{DIN} is estimated as 69.605 kg N km⁻² y⁻² for the average of 1999 and 2000 inputs (NO₃ + NH₄) as.

We assume that v_{DIN} is equal to v_{Sub} and v_{DIP}

I_{DIP} is estimated as 585.15 kg P km⁻² y⁻² by:

$$I_{DIP} = (1 - v_{DIP}) \times DIP_{output} \quad (S4)$$

We based our estimation of organic carbon, nitrogen and phosphorus inputs considering initial analysis of organic carbon in glacier forefield soils, chemical analyses of glacier meltwater (Hodson et al., 2005) and the ornithogenic contribution to soils (Jakubas et al., 2008; Ziolek and Melke, 2014), and used the stoichiometry from Bradley et al. (2015) and Bernasconi et al. (2011).

Final allochthonous inputs are as follows:

Table S2. Final allochthonous inputs

Variable	Annual input ($\mu\text{g } 1.19\text{cm}^{-2} \text{ y}^{-1}$)
DIN	8.283
ON ₁	20.790
ON ₂	48.540
S ₁	147.51
S ₂	344.19
OP ₁	12.240

OP ₂	28.560
DIP	69.633

Inputs are evenly spread over snowmelt and summer period (days 155 to 264), and through 20cm depth ($v = 0.17/20 = 0.0085$).

The sensitivity of microbial and nutrient dynamics to this allochthonous flux is the focus of future work, in which we hope to address the issues of uncertainty of external inputs and leaching.

The model is run for 120 years to encapsulate the entirety of the observational dataset. Annual forcings (Fig. S3) are repeated for the entire duration of the model run.

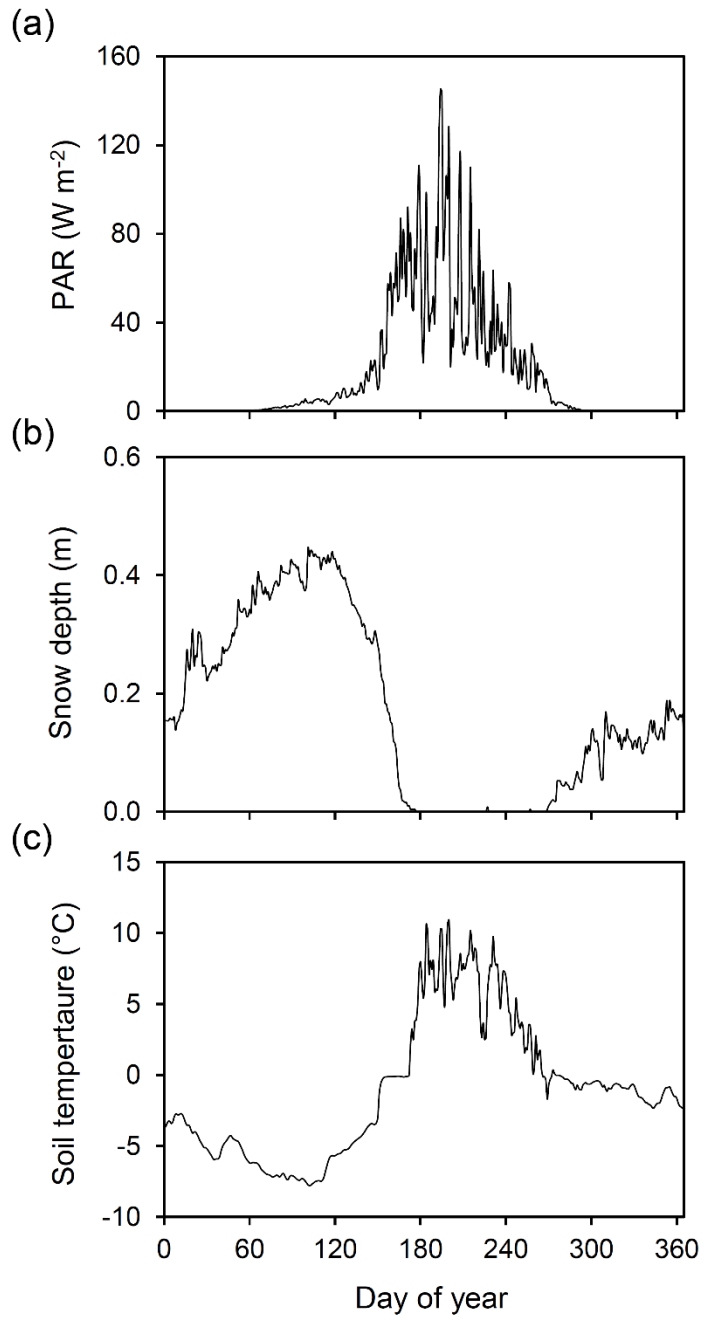


Fig. S3. Annual forcings.

S3.3. Table S3. Model parameters

Parameter	Description	Units	Value (Reference)
T_{ref}	Reference temperature for rates	°C	25 (<i>Frey et al., 2010</i>)
NC	C:N ratio (mass)	Unitless	0.141 (<i>Bernasconi et al., 2011</i>)
PC	C:P ratio (mass)	Unitless	0.083 (<i>Bernasconi et al., 2011</i>)
α_A	Death rate (autotrophs)	d ⁻¹	0.070 (<i>Bradley et al., 2015</i>)
α_H	Death rate (heterotrophs)	d ⁻¹	0.070 (<i>Bradley et al., 2015</i>)
ex_A	Exudates & EPS production (autotrophs)	Unitless	0.014 (<i>Allison, 2005</i>)
ex_H	Exudates & EPS production (heterotrophs)	Unitless	0.014 (<i>Allison, 2005</i>)
ρ_{Sub}	Slow-down of subglacial microbial growth rate	Unitless	0.2 (<i>Bradley et al., 2015</i>)
K_{Sub}	Lower half-saturation constants (K_S , K_N & K_P) for subglacial microbes	Unitless	0.8 (<i>Bradley et al., 2015</i>)
K_L	Light half-saturation constant for autotrophs (A_2 & A_3)	W m ⁻² (PAR)	11.88 (<i>De Nobel et al., 1998; Van Liere and Walsby, 1982; Chapra et al., 2014; Thornton et al., 2010; MacIntyre et al., 2002</i>)
K_S	Substrate half-saturation constant for heterotrophs	µg g ⁻¹	349 .00 (<i>Bradley et al, 2015</i>)
K_N	DIN half-saturation constant	µg g ⁻¹	49.21 (<i>stoichiometric</i>)

K_P	DIP half-saturation constant	$\mu\text{g g}^{-1}$	28.967 (<i>stoichiometric</i>)
n_f	Downscaling of Y and I_{max} when fixing nitrogen	Unitless	0.25 (<i>Bottomley and Myrold, 2007; LaRoche and Breitbarth, 2005; Breitbarth et al., 2008; Goebel et al., 2008</i>)
K_{N2}	Nitrogen fixation inhibition	$\mu\text{g g}^{-1}$	49.209 (<i>Bradley et al., 2015; Holl and Montoya, 2005; Rabouille et al., 2006</i>)
DIN_t	Threshold value of DIN for nitrogen fixation inhibition	$\mu\text{g g}^{-1}$	0
q	Proportion of necromass that becomes labile (S_1)	Unitless	0.3
J_{S1}	Bioavailability (preference) of S_1	Unitless	0.68 (<i>Bradley et al, 2015</i>)
J_{S2}	Bioavailability (preference) of S_2	Unitless	0.15 (<i>Bradley et al, 2015</i>)
g_{Sub}	Leaching of substrate	d^{-1}	0
g_{DIN}	Leaching of DIN	d^{-1}	0
g_{DIP}	Leaching of DIP	d^{-1}	0
d	Active fraction of microbial biomass	Unitless	0.285 (<i>Wang et al, 2014</i>)
V_{Sub}	Proportion of allochthonous substrate deposition retained	Unitless	0.0085
V_{DIN}	Proportion of allochthonous DIN deposition retained	Unitless	0.0085

V_{DIP}	Proportion of allochthonous DIP deposition retained	Unitless	0.0085
Parameter	Description	Units	Value determined in lab (Standard Error)
I_{maxH}	Maximum growth rate (heterotrophs)	d^{-1}	0.550 (0.027)
I_{maxA}	Maximum growth rate (autotrophs)	d^{-1}	0.550 (assumed)
Q_{10}	Temperature sensitivity	<i>Unitless</i>	2.91 (0.013)
Y_H	Growth efficiency (heterotrophs)	g carbon (g consumed) ⁻¹	0.060 (0.003)
Y_A	Growth efficiency (autotrophs)	g carbon (g consumed) ⁻¹	0.060 (assumed)

S4. Statistical significance test of lab measurements (ANOVA & Tukey)

Table S4. Bacterial carbon production

Difference between treatments	P-value
Low - High	0.064
Medium - High	0.488
None – High	0.100
Medium – Low	0.547
None – Low	0.994
None - Medium	0.697

Table S5. Growth rate

Difference between treatments	P-value
Low - High	0.952
Medium - High	0.093
None – High	0.067
Medium – High	0.261
None – Low	0.202
None - Medium	0.999

Table S6. Respiration

Difference between incubation temperatures	P-value
5°C - 25°C	2.6*10 ⁻⁶
Killed (autoclave) - 25°C	2.0*10 ⁻⁷
Killed (furnace) - 25°C	5.0*10 ⁻⁷
Killed (autoclave) - 5°C	0.464
Killed (furnace) - 5°C	0.764
Killed (furnace) – Killed (autoclave)	0.954

S5. Microbial diversity

NCBI Project ID: PRJNA341831

Table S7. Accession numbers

Accession number	Sample ID	Soil age (years)
SAMN05729451	S132101a	0
SAMN05729452	S132102a	0
SAMN05729453	S131101a	0
SAMN05729454	S132301a	29
SAMN05729455	S132303a	29
SAMN05729456	S132302a	29
SAMN05729457	S131301a	29
SAMN05729458	S133301a	29
SAMN05729459	S132503a	50
SAMN05729460	S132501a	50
SAMN05729461	S132502a	50
SAMN05729462	S131501a	50
SAMN05729463	S133501a	50
SAMN05729464	S132603a	113
SAMN05729465	S132602a	113
SAMN05729466	S132601a	113

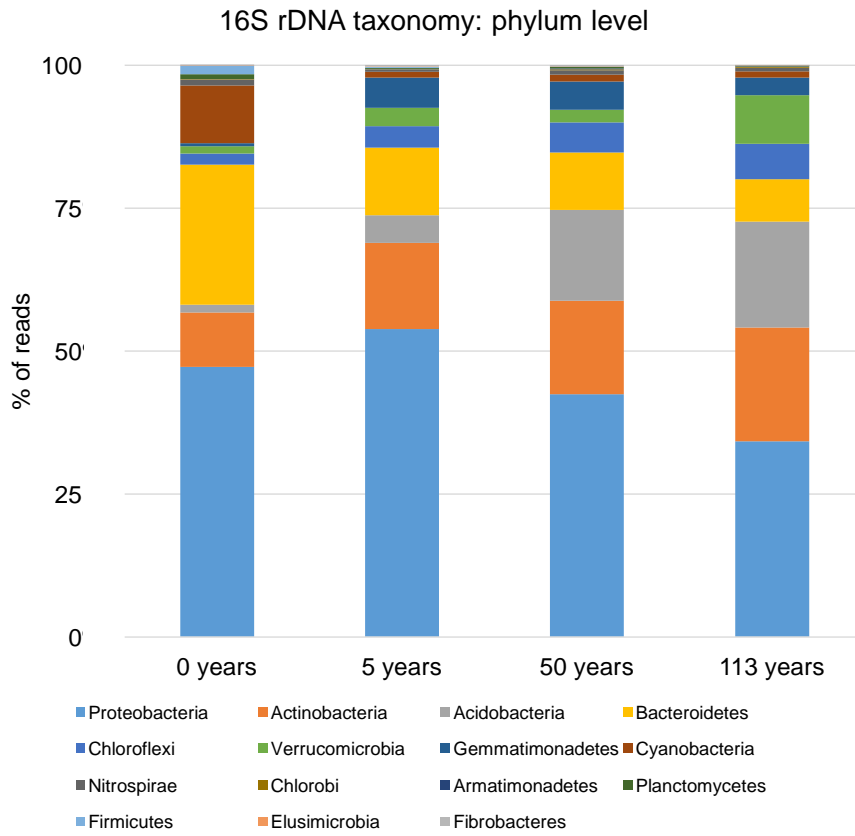


Fig. S4. Diversity of microbial distribution (phylum level) across the chronosequence, based on 16S rDNA taxonomy.

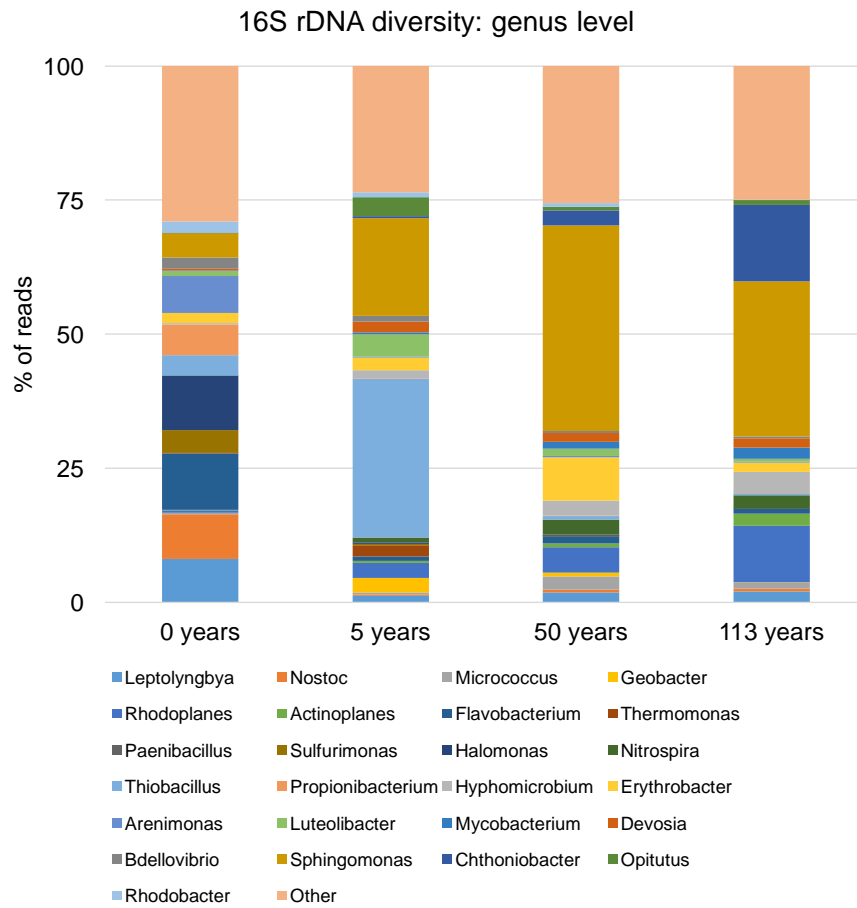


Fig. S5. Diversity of microbial distribution (genus level) across the chronosequence, based on 16S rDNA taxonomy.

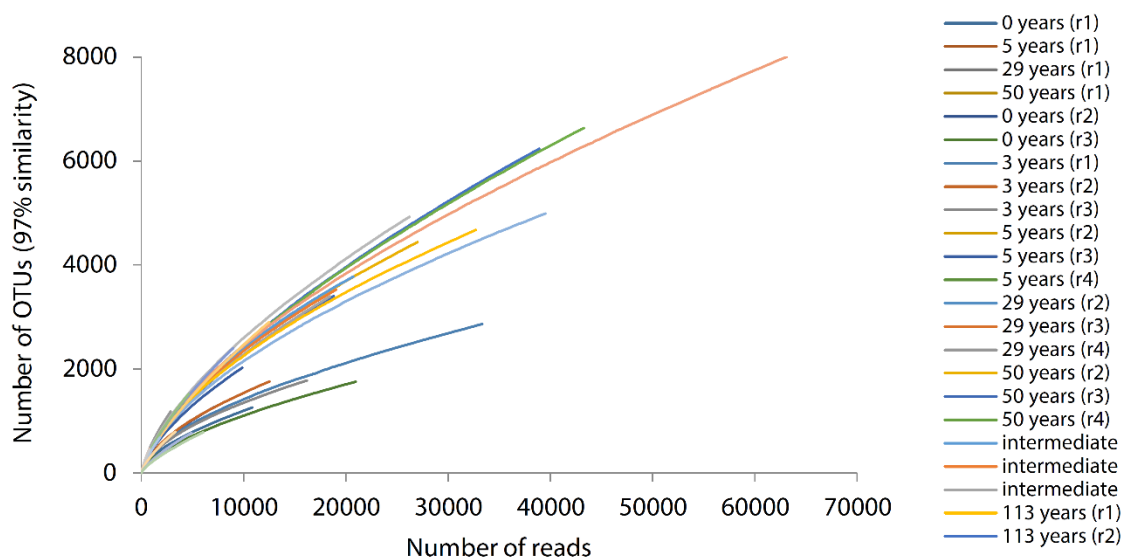


Fig. S6. Rarefaction curves for sequencing.

S6. References

- Allison, S. D.: Cheaters, diffusion and nutrients constrain decomposition by microbial enzymes in spatially structured environments, *Ecol Lett*, 8, 626-635, DOI 10.1111/j.1461-0248.2005.00756.x, 2005.
- Alves, R. J. E., Wanek, W., Zappe, A., Richter, A., Svenning, M. M., Schleper, C., and Urich, T.: Nitrification rates in Arctic soils are associated with functionally distinct populations of ammonia-oxidizing archaea, *Isme J*, 7, 1620-1631, 10.1038/ismej.2013.35, 2013.
- Bernasconi, S. M., Bauder, A., Bourdon, B., Brunner, I., Bunemann, E., Christl, I., Derungs, N., Edwards, P., Farinotti, D., Frey, B., Frossard, E., Furrer, G., Gierga, M., Goransson, H., Gulland, K., Hagedorn, F., Hajdas, I., Hindshaw, R., Ivy-Ochs, S., Jansa, J., Jonas, T., Kiczka, M., Kretzschmar, R., Lemarchand, E., Luster, J., Magnusson, J., Mitchell, E. A. D., Venterink, H. O., Plotze, M., Reynolds, B., Smittenberg, R. H., Stahl, M., Tamburini, F., Tipper, E. T., Wacker, L., Welc, M., Wiederhold, J. G., Zeyer, J., Zimmermann, S., and Zumsteg, A.: Chemical and Biological Gradients along the Damma Glacier Soil Chronosequence, Switzerland, *Vadose Zone J*, 10, 867-883, Doi 10.2136/Vzj2010.0129, 2011.
- Bottomley, P., and Myrold, D.: Biological N Inputs, in: *Soil microbiology, ecology and biochemistry*, 3 ed., edited by: Paul, E., Elsevier, USA, 2007.
- Bradley, J. A., Singarayer, J. S., and Anesio, A. M.: Microbial community dynamics in the forefield of glaciers, *Proceedings. Biological sciences / The Royal Society*, 281, 2793-2802, 10.1098/rspb.2014.0882, 2014.
- Bradley, J. A., Anesio, A. M., Singarayer, J. S., Heath, M. R., and Arndt, S.: SHIMMER (1.0): a novel mathematical model for microbial and biogeochemical dynamics in glacier forefield ecosystems, *Geosci. Model Dev.*, 8, 3441-3470, 10.5194/gmd-8-3441-2015, 2015.
- Bratbak, G., and Dundas, I.: Bacterial Dry-Matter Content and Biomass Estimations, *Appl Environ Microb*, 48, 755-757, 1984.
- Breitbarth, E., Wohlers, J., Klas, J., LaRoche, J., and Peeken, I.: Nitrogen fixation and growth rates of *Trichodesmium* IMS-101 as a function of light intensity, *Mar Ecol Prog Ser*, 359, 25-36, Doi 10.3354/Meps07241, 2008.

Chapra, S. C., Flynn, K. F., and Rutherford, J. C.: Parsimonious Model for Assessing Nutrient Impacts on Periphyton-Dominated Streams, *J Environ Eng*, 140, 10.1061/(Asce)Ee.1943-7870.0000834, 2014.

De Nobel, W. T., Matthijs, H. C. P., Von Elert, E., and Mur, L. R.: Comparison of the light-limited growth of the nitrogen-fixing cyanobacteria *Anabaena* and *Aphanizomenon*, *New Phytol*, 138, 579-587, DOI 10.1046/j.1469-8137.1998.00155.x, 1998.

Frey, B., Rieder, S. R., Brunner, I., Plotze, M., Koetzsch, S., Lapanje, A., Brandl, H., and Furrer, G.: Weathering-Associated Bacteria from the Damma Glacier Forefield: Physiological Capabilities and Impact on Granite Dissolution, *Appl Environ Microb*, 76, 4788-4796, Doi 10.1128/Aem.00657-10, 2010.

Goebel, N. L., Edwards, C. A., Carter, B. J., Achilles, K. M., and Zehr, J. P.: Growth and carbon content of three different-sized diazotrophic cyanobacteria observed in the subtropical North Pacific, *J Phycol*, 44, 1212-1220, DOI 10.1111/j.1529-8817.2008.00581.x, 2008.

Greenfell, T. C., and Maykut, G. A.: The optical properties of ice and snow in the Arctic basin, *J Glaciol*, 18, 18, 1977.

Hodson, A. J., Mumford, P. N., Kohler, J., and Wynn, P. M.: The High Arctic glacial ecosystem: new insights from nutrient budgets, *Biogeochemistry*, 72, 233-256, DOI 10.1007/s10533-004-0362-0, 2005.

Holl, C. M., and Montoya, J. P.: Interactions between nitrate uptake and nitrogen fixation in continuous cultures of the marine diazotroph *Trichodesmium* (Cyanobacteria), *J Phycol*, 41, 1178-1183, DOI 10.1111/j.1529-8817.2005.00146.x, 2005.

Jakubas, D., Zmudczynska, K., Wojczulanis-Jakubas, K., and Stempniewicz, L.: Faeces deposition and numbers of vertebrate herbivores in the vicinity of planktivorous and piscivorous seabird colonies in Hornsund, Spitsbergen, *Pol Polar Res*, 29, 45-58, 2008.

LaRoche, J., and Breitbarth, E.: Importance of the diazotrophs as a source of new nitrogen in the ocean, *J Sea Res*, 53, 67-91, DOI 10.1016/j.seares.2004.05.005, 2005.

MacIntyre, H. L., Kana, T. M., Anning, T., and Geider, R. J.: Photoacclimation of photosynthesis irradiance response curves and photosynthetic pigments in microalgae and cyanobacteria, *J Phycol*, 38, 17-38, DOI 10.1046/j.1529-8817.2002.00094.x, 2002.

Rabouille, S., Staal, M., Stal, L. J., and Soetaert, K.: Modeling the dynamic regulation of nitrogen fixation in the cyanobacterium *Trichodesmium* sp., *Appl Environ Microb*, 72, 3217-3227, Doi 10.1128/Aem.72.5.3217-3227.2006, 2006.

Van Liere, L., and Walsby, A. E.: Interactions of Cyanobacteria with Light, in: *The Biology of Cyanobacteria*, 2 ed., edited by: Whitton, B. A., and Carr, N. G., Blackwell Scientific, Oxford, 1982.

Ziolek, M., and Melke, J.: The impact of seabirds on the content of various forms of phosphorus in organic soils of the Bellsund coast, western Spitsbergen, *Polar Res*, 33, ARTN 19986 10.3402/polar.v33.19986, 2014.